Hutchinson-Gilford progeria syndrome mice display accelerated arterial thrombus formation and increased platelet reactivity

Yustina M. Puspitasari, Stefano Ministrini, Jiaying Han, Caroline Karch, Francesco Prisco, Luca Liberale, Susan Bengs, Alexander Akhmedov, Fabrizio Montecucco, Jürg H. Beer, Thomas F. Lüscher, Dario Bongiovanni, Giovanni G. Camici

Angaben zur Veröffentlichung / Publication details:

Puspitasari, Yustina M., Stefano Ministrini, Jiaying Han, Caroline Karch, Francesco Prisco, Luca Liberale, Susan Bengs, et al. 2024. "Hutchinson-Gilford progeria syndrome mice display accelerated arterial thrombus formation and increased platelet reactivity." *Thrombosis Research* 241: 109100. https://doi.org/10.1016/j.thromres.2024.109100.

Thrombosis Research 241 (2024) 109100

Contents lists available at ScienceDirect

Thrombosis Research

journal homepage: www.elsevier.com/locate/thromres

Full Length Article

Hutchinson-Gilford progeria syndrome mice display accelerated arterial thrombus formation and increased platelet reactivity

Yustina M. Puspitasari [a], Stefano Ministrini [a,b], Jiaying Han [c], Caroline Karch [a], Francesco Prisco [d], Luca Liberale [e,f], Susan Bengs [a], Alexander Akhmedov [a], Fabrizio Montecucco [e,f], Jürg H. Beer [a,g], Thomas F. Lüscher [a,h], Dario Bongiovanni [i,j], Giovanni G. Camici [a,k,*]

[a] Center for Molecular Cardiology, University of Zurich, Schlieren, Switzerland
[b] Internal Medicine, Angiology and Atherosclerosis, Department of Medicine and Surgery, University of Perugia, Perugia, Italy
[c] Department of Internal Medicine I, School of Medicine, University Hospital rechts der Isar, Technical University of Munich, Munich, Germany
[d] Laboratory for Animal Model Pathology, Institute of Veterinary Pathology, Vetsuisse Faculty, University of Zurich, Switzerland
[e] First Clinic of Internal Medicine, Department of Internal Medicine, University of Genoa, Genoa, Italy
[f] IRCCS Ospedale Policlinico San Martino Genoa – Italian Cardiovascular Network, Genoa, Italy
[g] Department of Internal Medicine, Cantonal Hospital of Baden, Baden, Switzerland
[h] Department of Cardiology, Royal Brompton & Harefield Hospitals, National Heart & Lung Institute, Imperial College, London, United Kingdom
[i] Department of Internal Medicine I, Cardiology, University Hospital Augsburg, University of Augsburg, Augsburg, Germany
[j] Department of Cardiovascular Medicine, Humanitas Clinical and Research Center IRCCS and Humanitas University, Rozzano, Milan, Italy
[k] Department of Research and Education, University Hospital Zurich, Zurich, Switzerland

ARTICLE INFO

Keywords:
Progeria
Arterial thrombosis
Hemostasis
Platelet
Lamin A

ABSTRACT

Introduction: Hutchinson-Gilford Progeria Syndrome (HGPS) is an ultra-rare premature aging genetic disorder caused by a point mutation in the lamin A gene, *LMNA*. Children with HGPS display short lifespans and typically die due to myocardial infarction or ischemic stroke, both acute cardiovascular events that are tightly linked to arterial thrombosis. Despite this fact, the effect of the classic HGPS *LMNA* gene mutation on arterial thrombosis remains unknown.

Methods: Heterozygous $Lmna^{G609G}$ knock-in ($Lmna^{G609G/+}$) mice, yielding an equivalent classic mutation observed in HGPS patients (c.1824C>T; pG608G mutation in the human *LMNA* gene) and corresponding wild-type (WT) control littermates underwent photochemically laser-induced carotid injury to trigger thrombosis. Coagulation and fibrinolytic factors were measured. Furthermore, platelet activation and reactivity were investigated.

Results: $Lmna^{G609G/+}$ mice displayed accelerated arterial thrombus formation, as underlined by shortened time to occlusion compared to WT littermates. Levels of factors involved in the coagulation and fibrinolytic system were comparable between groups, while $Lmna^{G609G/+}$ animals showed higher plasma levels of thrombin-antithrombin complex and lower levels of antithrombin. Bone marrow analysis showed larger megakaryocytes in progeric mice. Lastly, enhanced platelet activation upon adenosine diphosphate, collagen-related peptide, and thrombin stimulation was observed in $Lmna^{G609G/+}$ animals compared to the WT group, indicating a higher platelet reactivity in progeric animals.

Conclusions: LMNA mutation in HGPS mice accelerates arterial thrombus formation, which is mediated, at least in part, by enhanced platelet reactivity, which consequently augments thrombin generation. Given the wide spectrum of antiplatelet agents available clinically, further investigation is warranted to consider the most suitable antiplatelet regimen for children with HGPS to mitigate disease mortality and morbidity.

* Corresponding author at: Center for Molecular Cardiology, University of Zurich, Wagistrasse 12, CH-8952 Schlieren, Switzerland.
E-mail address: giovanni.camici@uzh.ch (G.G. Camici).

https://doi.org/10.1016/j.thromres.2024.109100
Received 18 December 2023; Received in revised form 12 July 2024; Accepted 17 July 2024
Available online 18 July 2024

1. Introduction

Arterial thrombosis is well recognized as a critical factor underlying age-related major adverse cardiovascular (CV) events [1]. Such thrombotic events are commonly initiated by atherosclerotic plaque erosion or rupture, exposing underlying vascular structures or necrotic core components to the circulation, thus driving the activation of the hemostatic process [2], or are embolic in nature in the context of atrial fibrillation or myocardial infarction. The acute formation of arterial intraluminal blood clots involves the interplay between vascular endothelium, platelets, and coagulation factors, counterbalanced by the fibrinolytic system. Despite being highly regulated, an imbalance between prothrombotic and antithrombotic factors may occur, thus preceding the formation of an occluding arterial thrombus and consequent ischemic damage to the downstream parenchyma [3].

Hutchinson-Gilford progeria syndrome (HGPS) is a rare genetic disease with striking features of premature aging caused by an autosomal dominant mutation in the nuclear lamin A gene. The majority of HGPS patients carry a heterozygous point mutation in exon 11 (c.1842C>T; p.G608G). This mutation activates a cryptic splicing donor site, leading to the production of truncated prelamin A with an internal deletion of 50 amino acids at the ZMPSTE24 cleavage site, known as progerin, which cannot undergo further processing to mature Lamin A [4,5]. Children with HGPS are phenotypically characterized by growth impairment, alopecia, subcutaneous fat loss, bone and joint abnormalities, and cardiovascular alterations, including premature and severe atherosclerosis [4,6]. HGPS patients die prematurely, typically at around 14 years of age, due to CV complications, including myocardial infarction and ischemic stroke. To date, myocardial infarction and ischemic stroke in HGPS patients are attributed to severe atherosclerosis [7]. On the other hand, both myocardial infarction and ischemic stroke are mediated by acute arterial thrombosis events [8]. Whether this specific laminopathy disorder results in an alteration in arterial thrombus formation remains unknown.

In this study, we investigated the effect of a specific lamin A gene mutation typically observed in HGPS patients on arterial thrombus formation and on the components of the hemostasis system. To this end, we performed an *in vivo* endothelial-specific injury to trigger arterial thrombosis on a murine model of HGPS.

2. Methods

2.1. Animals

28–30-week-old heterozygous *Lmna*^{G609G} knock-in animals (*Lmna*$^{G609G/+}$) of both sexes and the corresponding wild-type (WT) littermate controls were used for all experiments. The *Lmna*^{G609G} (c.1827C>T; p.G609G) knock-in mouse model was a generous gift from Professor Carlos-Lopez Otin, Departemento de Bioquimica y Biologia Molecular, University of Oviedo, Spain. The transgenic mice were generated on C57BL/6 background as described previously and expressed the murine endogenous *LMNA* gene fostering the corresponding classic mutation of patients with HGPS (c.1824C>T; pG608G) [4]. Mice experimental age was chosen as the optimal time point when *Lmna*$^{G609G/+}$animals have a clearly pathologic phenotype, but not yet in the terminal state, according to the previous descriptions of this transgenic mouse model [5].

All animals were kept in a temperature-controlled animal facility under a normal light/dark cycle with free access to food and water. All procedures were approved by the Cantonal Veterinary Authority of Zurich, Switzerland (ZH171/2021). Animal experiments were performed conform to the Directive 2010/63/EU of the European Parliament and of the Council of 22 September 2010 on the protection of animals used for scientific purposes.

2.2. Genotyping

DNA was extracted from the ear tissue punched at weaning- DNA was amplified using KAPA Mouse Genotyping kit (KK7301, Merck, Darmstadt, Germany) following the manufacturer's recommendation. PCR was performed using previously published oligonucleotides: 5′-AAGGGGCTGGGAGGACAGAG-3′ and 5′-AGCATGCAATAGGGTGG AAGGA-3′. A 3 min denaturation step at 95 °C was followed by 36 cycles at 95 °C for 15 s, 65 °C for 10 s, and 72 °C for 10 s and completed by a final extension for 1 min at 72 °C and 25 °C for 5 min. The PCR fragment consisted of 240 bp for the mutant allele and 100 bp for the wild-type allele.

2.3. In vivo laser-induced carotid artery thrombosis model

Lmna$^{G609G/+}$ and WT control mice underwent photochemical injury of the common carotid artery CCA as previously described [9–11]. Briefly, mice were anesthetized by intraperitoneal injection of 50 mg/kg of body weight (BW) sodium pentobarbital (Butler, Columbus, OH, USA) and the depth of anesthesia was confirmed by the absence of twitch reflex response. Rose Bengal (Fischer Scientific, Fair Lawn, NJ, USA) was dissolved in phosphate buffer saline to reach a concentration of 12 mg/mL and then injected intravenously through the tail vein with a dose of 62.6 mg/kg BW. Mice were placed and fixed in a supine position under a dissecting microscope, and a midline cervical incision was made to expose the right common carotid artery. To assess the carotid blood flow, a Doppler flow probe (Model 0.5 VB, Transonic Systems, Ithaca, NY, USA) connected to a flowmeter (Model T106, Transonic Systems, Ithaca, NY, USA) was placed inclosing the right carotid artery. Within five to ten minutes after Rose Bengal injection, a 1.5 mW green light laser (540 nm; Melles Griot, Carlsbad, CA, USA) was applied to the right carotid artery as the site of injury at a distance of 6 cm for 60 min or until total occlusion occurred. Carotid blood flow, cyclic flow variations, and heart rate were continuously recorded from the onset of injury until occlusion. Total occlusion was defined as carotid blood flow below 0.1 mL/min for at least 1 min. Carotid artery time-to-occlusion (TTO) is the time lapse between the application of the laser beam and the total occlusion of the carotid. Thrombus embolization was defined as an increase of blood flow above 0.1 mL/min after a previous decrease below said level lasting <1 min. The number of embolization episodes is a readout of fibrinolysis efficacy [9–11].

2.4. Blood cell count

Total blood cell count was performed on a ScilVet ABCplus (Horiba, Kyoto, Japan) using citrate-anticoagulated blood collected from animals that were not exposed to the carotid artery thrombosis procedure.

2.5. Determination of plasminogen activator inhibitor-1 and tissue factor levels and activity in arterial samples

Uninjured contralateral carotid arteries were lysed (50 mmol/L Tris–HCl, 100 mmol/L NaCl, 0.1 % Triton X-100, pH 7.4), and total protein concentration was determined by Bradford protein assay according to the manufacturer's recommendations (VWR Life Science AMRESCO, Solon, OH, USA). Tissue factor (TF) and plasminogen activator inhibitor-1 (PAI-1) arterial expressions were measured in arterial lysates using colorimetric enzyme-linked immunosorbent assay (DY3178 and DY3828 respectively; R&D system, Minneapolis, MN, USA). Both TF and PAI-1 levels were normalized to the measured protein concentration.

TF activity was determined using colorimetric ACTICHROME ® TF assay following the manufacturer's instructions as previously described (846; American Diagnostica, Stamford, CT, USA) [10,11]. Briefly, arterial lysates were mixed with factor VIIa and X to form the TF/FVIIa complex and converted factor X to Xa. Factor Xa subsequently cleaves

the chromogenic substrate SPECTROZYME FXa, which releases para-nitroanilin chromophores. The optical density of cleaved SPECTROZYME FXa was determined at 405 nm by Nanodrop 2000 Spectrophotometer (Thermo Scientific, Waltham, MA, USA). Finally, TF (pM) content was calculated according to a standard curve. TF activity detected by the colorimetric assay was normalized to the total protein content of the sample and expressed as pmol/g of total protein.

2.6. Western blotting

Protein expression was determined by Western blot analysis as previously described [12]. Mouse aortas were homogenized in lysis buffer (Tris 50 mM, NaCl 150 mM, EDTA 1 mM, NaF 1 M, DTT 1 mM, aprotinin 10 mg/mL, leupeptin 10 mg/mL, Na3VO4 0.1 mM, phenylmethylsulfonyl fluoride (PMSF) 1 mM, and NP-40 0.5 %). Protein concentration was determined using Bradford protein assay according to the manufacturer's recommendation (PanReac Applichem, Darmstadt, Germany). 15 μg of protein lysates were separated on 10 % SDS–PAGE gels and transferred to a polyvinylidene fluoride membrane using a wet-transfer method. Membranes were incubated with primary antibodies against Collagen 3A1 (1:2500, Santa Cruz Biotechnology, CA, USA), Lamin A/C (1:1000, Santa Cruz Biotechnology, CA, USA), and glyceraldehyde 3-phosphate dehydrogenase (GAPDH) (1:40000, Merck Millipore, Billerica, MA, USA) at 4 °C overnight on a shaker. The following incubation with secondary antibodies (Southern Biotechnology, Birmingham, AL, USA) was done for one hour at room temperature. Densitometric analyses were performed (Amersham Imager 600, GE Healthcare Europe GmbH, Glattbrugg, Switzerland), and protein expression was normalized to GAPDH.

2.7. Enzyme-linked immunosorbent assays

Blood was collected *via* intracardiac puncture and immediately mixed with ethylenediaminetetraacetic acid (EDTA). The EDTA-blood solution was centrifuged for 15 min at 3000*g*, as previously described [9]. Plasma was collected and snap-frozen in liquid nitrogen. Levels of proteins of interest were measured using colorimetric enzyme-linked immunosorbent assays species-specific following the manufacturer's instruction. Specifically, DY3178 was used for TF (R&D systems, Minneapolis, MN, USA), ab233615 was used for tissue-plasminogen activators (tPA; Abcam, Cambridge, UK), DY3828 was used for plasminogen activator inhibitor 1 (R&D systems, Minneapolis, MN, USA), abx258705 was used for D-dimer (Abbexa, Cambridge, UK), MPS00 was used for soluble P-selectin (R&D systems, Minneapolis, MN, USA), NBP2–68171 was used for von Willebrand factor (vWF; Novus Biologicals, Cambridge, UK), NBP2–60632 was used for antithrombin III (Novus Biologicals, Cambridge, UK), and ab137994 was used for thrombin-antithrombin complexes (Abcam, Cambridge, UK).

2.8. Flow cytometry analysis of platelet reactivity and platelet receptor density

Washed platelets were isolated as previously described and used for all flow cytometry-based platelet analysis [10,13,14]. Blood was collected into 0.1 M sodium citrate and centrifuged at 200 *g* for 8 min without brakes. Afterward, plasma was transferred into 15 mL tubes and incubated for 10 min at 37 °C with the addition of 0.02 U Apyrase/mL (A6535; Sigma-Aldrich, Missouri, USA) and 1 μL/mL prostaglandin E1 (538,903; Merck, Darmstadt, Germany) as described before [10]. After a second round of centrifugation at 800 *g* for 15 min (no brakes), pellets were resuspended in modified Tyrodes-HEPES buffer (5 mM HEPES, 137 mM NaCl, 0.42 mM NaH_2PO_4, 2 mM KCl, 12 mM $NaHCO_3$, 5.5 mM glucose, 0.35 % bovine serum albumin, pH 7.35) and washed at 1300 g for 5 min with the presence of 1 μL/mL prostaglandin E1. Pelleted platelets were resuspended in modified Tyrodes-HEPES buffer and supplied with 1 mM $CaCl_2$ and 1 mM $MgCl_2$.

For platelet reactivity assay, washed platelets were stimulated with adenosine diphosphate (ADP) (10 μM; 01905; Sigma-Aldrich, St. Louis, MO, USA), CRP (20 μg/mL; CRP-XL; Cambcol, Littleport, UK), and thrombin (0.1 U/mL; T6884; Merck, Darmstadt, Germany) at room temperature. Agonists' concentrations were specified according to our preliminary tests and established *ex vivo* platelet aggregation assay [11,15,16]. In parallel with stimulation, platelets were stained with anti-mouse antibodies CD41 (BioLegend, San Diego, CA, USA), P-Selectin (CD62P) (eBioscience, San Diego, CA, USA)and activated GPIIb/IIIa (JON/A) (EMFRET Analytics, Würzburg, Germany). For membrane phosphatidylserine detection, washed platelets were double stimulated with Thrombin and CRP using the same concentration mentioned above and incubated with fluorescently labeled annexin V (BioLegend, San Diego, CA, USA). Meanwhile, washed platelets were kept unstimulated at room temperature for baseline platelet receptor quantification. Platelets were stained with anti-mouse antibodies against CD41, GPIa (EMFRET Analytics, Würzburg, Germany), and GPIbα (EMFRET Analytics, Würzburg, Germany). Anti-mouse antibodies against GPVI (EMFRET Analytics, Würzburg, Germany) were used to detect GPVI surface receptors at baseline and after stimulation with CRP to detect shedding. Details regarding the antibody dilutions and reference numbers are listed in Table S1. After incubation in the dark for 30 min, samples were analyzed immediately with flow cytometry. Results were analyzed with FlowJo analysis software (BD BioScience, Ashland, OR, USA). After excluding doubles (with FSC-W/FSC-A plots) and gating for platelet size, only CD41-positive cells were included in the analysis. Mean Fluorescence Intensity (MFI) was analyzed.

2.9. Platelets protein extraction

Platelets-rich plasma (PRP) was obtained by centrifugation as described above, then diluted 1:1 with a wash buffer solution (10 mM sodium citrate, 150 mM NaCl, 1 mM EDTA, 1 % (w/v) dextrose, pH 7.4) in a 15 mL tube with the addition of 1 μL/mL prostaglandin E1 before incubating at 37 °C for 10 min. Afterwards, 1 μL/mL prostaglandin E1 was added and centrifuged at 800 *g* for 15 min (no brakes). The supernatant was removed, and the pellet was resuspended in 200 μL wash buffer with the addition of 1 μL/mL prostaglandin E1, then incubated at 37 °C for 5 min. The supernatant was discarded and the pellet was resuspended in a 1:1 solution of Tyrodes-HEPES buffer (see above) without bovine serum albumin and platelets lysis buffer (2 % NP-40, 30 mM HEPES, 150 mM NaCl, 2 mM EDTA, 1 mM sodium fluoride, 1 mM 1,4-dithiothreitol, 10 mg/mL aprotinin, 10 mg/mL leupeptin, 0.1 mM Na3VO4, 1 mM phenylmethylsulfonyl fluoride, pH 7.4) for 20 min, before proceeding with protein concentration measurement and Western Blot, as described above.

2.10. Bone marrow histopathology

Femurs from $Lmna^{G609G/+}$ and WT control mice were collected shortly after euthanasia, fixed in 4 % paraformaldehyde for 24 h, and transferred into 70 % ethanol until embedded in paraffin. Three-microns thick consecutive sections were stained with hematoxylin and eosin and immunohistochemistry (IHC). IHC was performed using the horseradish peroxidase (HRP) method to detect Integrin β3 (CD61). After deparaffination, sections underwent antigen retrieval in EDTA buffer (pH 9.0) for 20 min at 98 °C, followed by incubation with monoclonal rabbit anti-Integrin β3 antibody (D7X3P, Cell Signaling Technology, Danvers, USA) at 1:400 (diluted in dilution buffer, Agilent Dako, Santa Clara, USA) for 1 h at room temperature (RT). This was followed by the blocking of endogenous peroxidase (peroxidase block, Agilent Dako) for 10 min at RT, incubation with Envision-HRP Rabbit detection system (Agilent Dako) for 30 min at RT, and incubation with AEC (Zytomed Systems GmbH, Berlin, Germany) for 10 min in Autostainer Link 48 (Agilent Dako). Sections were subsequently counterstained with hematoxylin. The sections were examined by a board-certified veterinary pathologist

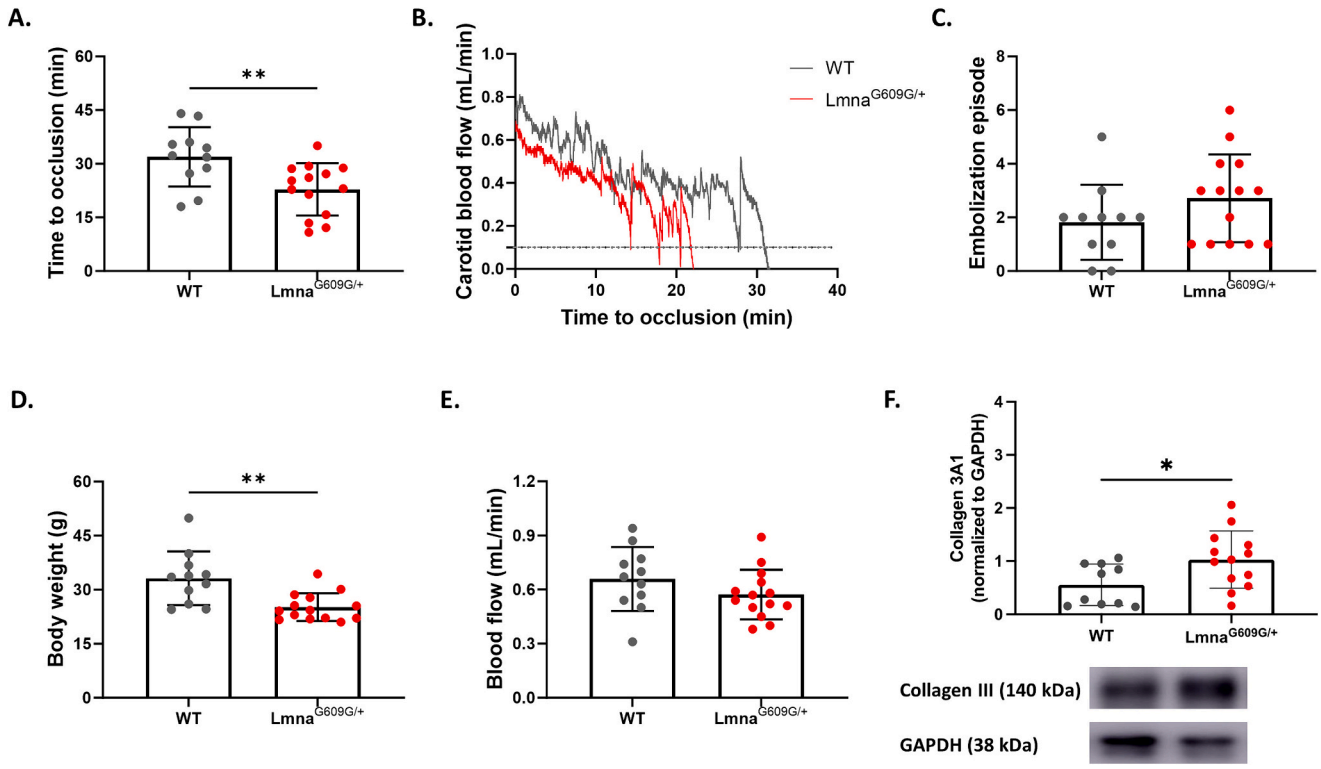

Fig. 1. *In vivo* carotid arterial thrombosis in a mouse model of Hutchinson-Gilford progeria syndrome (A) *Lmna*$^{G609G/+}$ mice showed accelerated formation of an occlusive thrombus in their carotid artery following laser-induced endothelial injury as compared to the control group. (B) Representative trace of mean blood flow of both groups until occlusion occurred (mean flow ≤0.1 mL/min for at least 1 min). (C) The number of thrombus embolization episodes is comparable between groups of animals. (D) *Lmna*$^{G609G/+}$ mice had lower body weight compared to the wild-type (WT), yet (E) no difference in initial blood flow was detected between *Lmna*$^{G609G/+}$ mice and WT littermates. (F) Compared to the WT littermates, *Lmna*$^{G609G/+}$ mice displayed a higher expression of collagen III in their vascular tissue. n = 11–14 different animals per group. Results are evaluated by unpaired two-tailed Student's t-test. Results are presented as mean ± SD. *$P < 0.05$; **$P < 0.01$.

in a blinded fashion. Morphological changes were quantitatively assessed using the Visiopharm 2023.09.3.15043 software (Visiopharm, Hoersholm, Denmark). For each section, the bone marrow of the femur was manually outlined and annotated as a region of interest (ROI), manually excluding artefactually altered areas. An APP (Analysis Protocol Package), based on a threshold method, was designed in Visiopharm and run on each ROI to measure its total area (μm^2) as well as the area, the number and the lesser diameter (minimum Feret's diameter) of the Integrin β3-positive elements (megakaryocytes; MK). The percentage of positive area, expressed as the ratio between the classified area and the total ROI area, was obtained for each animal according to the following formula: ([classified area (μm^2)]/[ROI area (μm^2)]) × 100. The number of MK, expressed as the ratio between the total number of MK and the total ROI area, was obtained for each animal according to the following formula: ([total MK number)]/[ROI area (μm^2) × 10^{-6}]).

2.11. Statistical analysis

Data are expressed as mean ± SD. All statistical analyses were performed using GraphPad Prism 10 software (GraphPad Software, Inc., La Jolla, CA). Data normal distribution was initially confirmed with the Kolmogorov-Smirnov normality test. For dual comparisons, normal data were statistically analyzed with a two-tailed unpaired student t-test. Two-way ANOVA with Sidak's *post hoc* test was applied for the analysis of platelet stimulation experiments. A p-value <0.05 was considered statistically significant.

3. Results

3.1. Progeric mice show accelerated arterial thrombotic occlusion

To investigate the effect of specific *LMNA* gene mutation, photochemical laser-induced carotid endothelial injury was performed in *Lmna*$^{G609G/+}$ mice and WT control littermates.

Carotid artery TTO was significantly reduced in *Lmna*$^{G609G/+}$ animals of both sexes, compared to the control group ($p < 0.01$, Fig. 1A-B), without significant differences in the embolization episodes (Fig. 1C). In the *post hoc* analysis, the observed reduction in TTO was not significantly influenced by the sex of the animals (Suppl. Fig. 1). As previously reported, *Lmna*$^{G609G/+}$ animals displayed slower growth rates, attained lower body weight ($p < 0.01$, Fig. 1D), and expressed more collagen III in their aorta compared to WT littermates [4,5,17]. ($p < 0.05$, Fig. 1F). Nevertheless, the initial carotid blood flow was comparable between the two groups. (Fig. 1E).

3.2. LMNA^{G609G} mutation does not affect the activation of the coagulation cascade and fibrinolytic pathway

To comprehensively clarify the molecular mechanisms underlying the findings described above, we explored pathways implicated in primary hemostasis (*i.e.*, platelet activation and aggregation), secondary hemostasis (*i.e.*, extrinsic coagulation pathway and fibrinolysis), and the cross-pathway between these two processes.

The coagulation cascade involves the activation of a series of clotting factors, and the extrinsic pathway is triggered by TF exposure following vessel injury [18]. This process is physiologically counterbalanced by

the fibrinolytic system, in which a disruption in the delicate balance between these two processes may lead to the development of pathologic thrombi [19,20]. In this study, the levels of TF in the plasma and arterial tissues did not differ between WT and *Lmna*$^{G609G/+}$ mice (Fig. 2A-B). Consistently with this finding, arterial TF factor activity was comparable in both groups (Fig. 2C). Meanwhile, levels of tPA – one of the crucial factors in the fibrinolytic system that converts plasminogen to plasmin – and its inhibitor, PAI-1, did not differ between *Lmna*$^{G609G/+}$ and WT mice (Fig. 2D-F). In addition, *Lmna*$^{G609G/+}$ and WT mice displayed comparable plasma levels of D-dimers, the fibrin degradation product, suggesting identical fibrinolysis processes (Fig. 2G).

3.3. Platelets from progeric mice possess higher platelet reactivity

We investigated the effect of *LMNA*^{G609G} mutation on platelet function and levels of von Willebrand factor (vWF), a crucial player in platelet adhesion to the injured site and platelet aggregation [21]. Complete blood count analysis revealed that platelet numbers and size, indicated by mean platelet volume, were not different between *Lmna*$^{G609G/+}$ mice and WT controls (Suppl. Fig. 2). Lamin A was expressed in platelets of both groups, with a lower intensity in *Lmna*$^{G609G/+}$ mice compared to WT, although not significantly different (Suppl. Fig. 2). Platelets isolated from both groups of animals also showed equal expression of platelet receptors, including GPIa, GPIbα, and GPVI in the resting state (Fig. 3A-C). Upon stimulation with CRP, GPVI receptor shedding was observed, with platelets from *Lmna*$^{G609G/+}$ mice showing higher GPVI cleavage compared to the WT littermates (Fig. 3D). Upon stimulation with both CRP and thrombin, platelets from *Lmna*$^{G609G/+}$ mice showed a significantly higher Annexin V signal compared to WT littermates, suggesting augmented phosphatidylserine externalization (Fig. 3E).

To assess platelet reactivity, *ex vivo* platelet function was assessed by flow cytometry after stimulation with different activators: ADP, collagen, and thrombin. Activation of platelets was assessed as changes in the expression of two activation markers, P-selectin (CD62P) and the activated form of the GPIIb/IIIa (JON/A) receptor. Washed platelets from *Lmna*$^{G609G/+}$ and WT mice showed similar expression of both platelet activation markers at baseline. Interestingly, upon activation with collagen, platelets from *Lmna*$^{G609G/+}$ mice displayed greater platelet activation as compared to the WT animals, as demonstrated by the significantly upregulated expression of both P-selectin and JON/A ($p < 0.05$, Fig. 4A, D-E). Similar results were obtained upon stimulation with thrombin ($p < 0.0001$, Fig. 4A, F-G). Higher platelet reactivity was also detected on platelets from *Lmna*$^{G609G/+}$ animals upon ADP stimulation but restricted to the marker JON/A only and not P-selectin (Fig. 4A-C). Nevertheless, circulating levels of soluble P-selectin and vWF in *Lmna*$^{G609G/+}$ animals did not differ from the WT littermates. (Suppl. Fig. 3A-B).

3.4. Progeric mice show larger megakaryocytes in the bone marrow

As a possible explanation for the above-described abnormal platelets reactivity, we investigated whether *LMNA* mutation morphologically affects megakaryopoiesis. The bone marrow of progeric animals displays a higher number and a larger total area of megakaryocytes, although in a not significant manner (Fig. 5A-C). However, megakaryocytes of animals bearing the *LMNA* mutation were significantly larger compared to WT littermates ($P < 0.05$, Fig. 5D).

3.5. *LMNA*^{G609G} mutation increases thrombin generation upon endothelial-specific injury

Thrombin is a central enzyme in arterial thrombosis involved in the intrinsic link between primary and secondary processes, given its function in converting fibrinogen to fibrin and activating platelets to eventually form stable hemostatic clots [22,23]. Therefore, to investigate whether thrombin was involved in the observed accelerated thrombus formation in the progeric animals, levels of the thrombin-antithrombin (TAT) complex were measured as a surrogate marker for thrombin generation in both groups of animals [24]. Animals bearing *LMNA*^{G609G} mutation displayed significantly higher circulating TAT complex levels compared to their WT littermates ($p < 0.05$, Fig. 6A). Furthermore, we also observed that the levels of antithrombin III – thrombin inhibitor – were lower in *Lmna*$^{G609G/+}$ compared to the control group ($p < 0.05$, Fig. 6B).

4. Discussion

This study provides the first experimental evidence of the deleterious effect of a specific laminopathy in regulating arterial thrombosis *in vivo*. We demonstrate that occluding arterial thrombosis triggered by endothelial-specific injury is accelerated in mice bearing an equivalent targeted HGPS classic *LMNA* mutation observed in HGPS patients. The specific *LMNA* mutation did not affect the extrinsic coagulation and the fibrinolytic pathway, yet it increased platelet reactivity upon stimulation. Furthermore, the *LMNA* mutation increased thrombin generation,

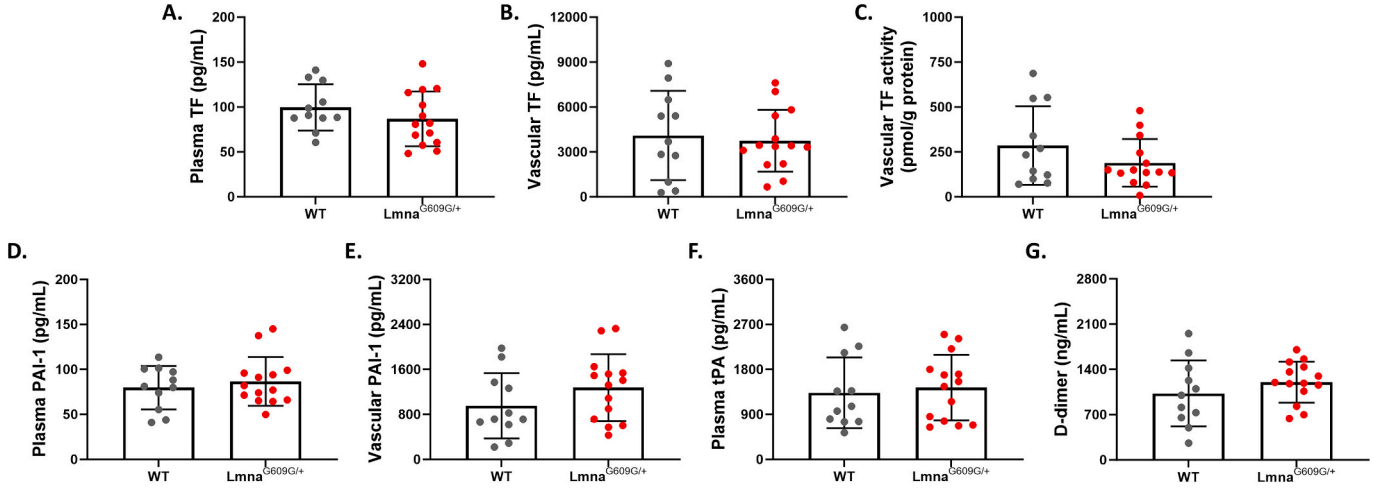

Fig. 2. Effect of *LMNA*^{G609G} mutation on extrinsic coagulation pathway and fibrinolytic system. HGPS classic *LMNA*^{G609G} mutation did not affect the levels and activity of tissue factor (TF) both in the (A) circulation and (B—C) vascular tissue. The fibrinolytic system was also unaltered in HGPS as compared to the wild-type group, as shown by the comparable levels of fibrinolytic mediators (D-E) plasminogen activator inhibitor-1 (PAI-1), (F) tissue plasminogen activator (tPA), and (G) plasma D-dimer. n = 11–14 different animals per group. Results are evaluated by unpaired two-tailed Student's t-test. Results are presented as mean ± SD.

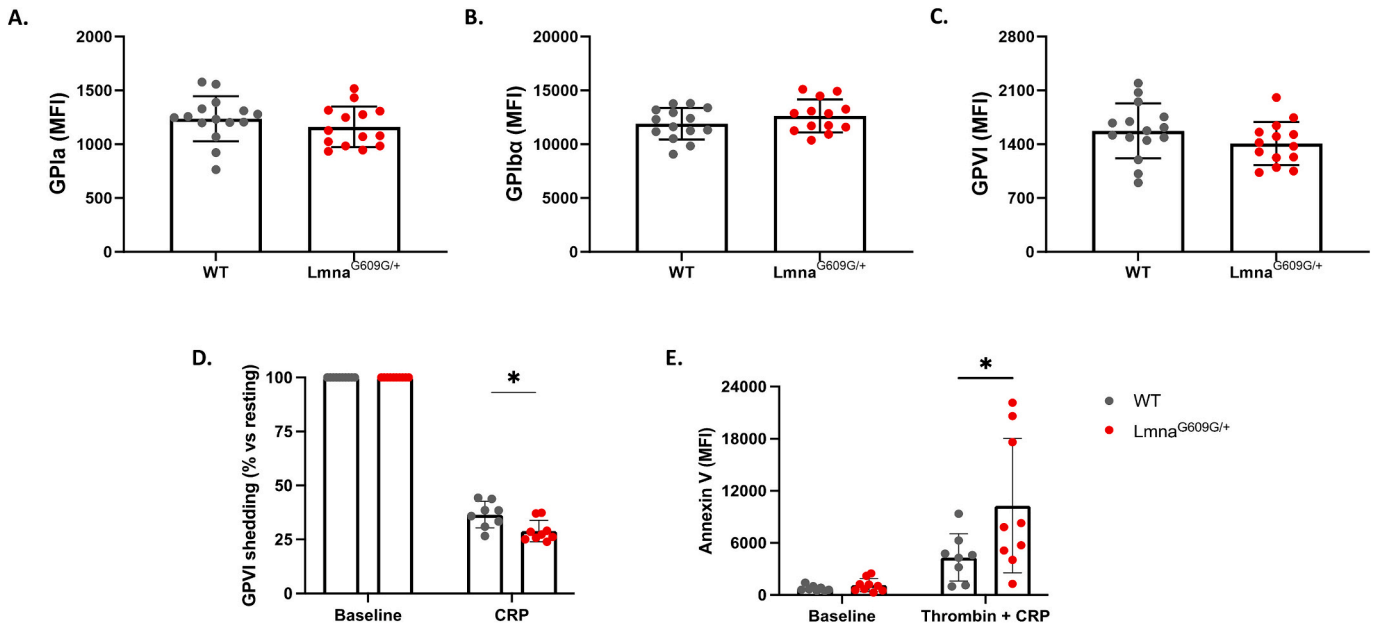

Fig. 3. Platelet receptors density on platelets of *Lmna*$^{G609G/+}$ and wild-type (WT) mice. *Lmna*$^{G609G/+}$ and WT mice displayed comparable densities of several platelet receptors, namely (A) glycoprotein Ia (GPIa), (B) GPIb, and (C) GPVI in the resting state. $n = 13$–15 different animals per group. Results are evaluated by unpaired two-tailed Student's t-test. (D) Meanwhile, *Lmna*$^{G609G/+}$ mice showed higher GPVI receptors shedding upon CRP stimulation compared to the control group. (E) Double-stimulated *Lmna*$^{G609G/+}$ platelets showed significantly higher expression of Annexin V, indicating higher phosphatidylserine externalization. $n = 8$–9 different animals per group. Results are evaluated by two-way ANOVA with Sidak's *post hoc* test. Results are presented as mean ± SD. $^{*}P < 0.05$.

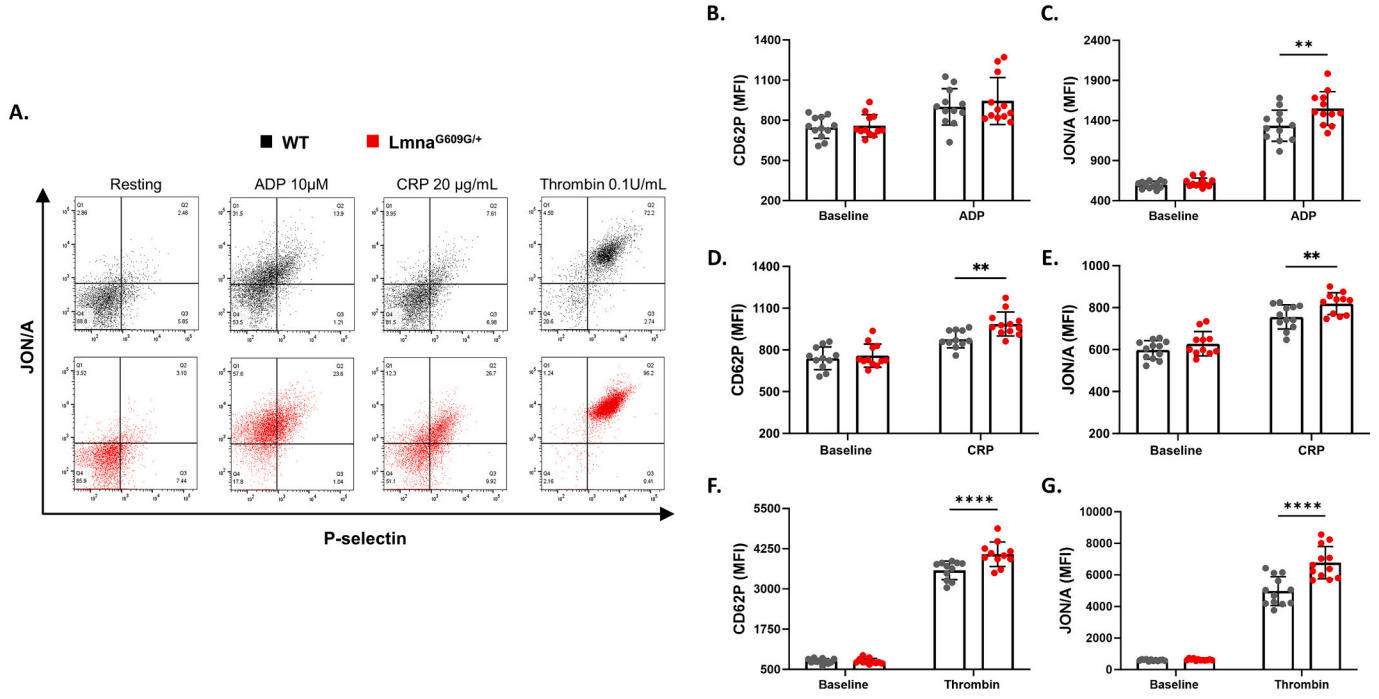

Fig. 4. Effect of *LMNA*^{G609G} mutation on *ex vivo* platelet activation. (A) Representative flow cytometric plots of resting and activated platelets upon stimulation with adenosine diphosphate (ADP), collagen, and thrombin. Mean fluorescence intensity (MFI) of platelet P-selectin (CD62P) and active integrin αIIbβ3 (JON/A) at resting state and after stimulation with the different stimulators. (B-G) In the resting state, platelets from *Lmna*$^{G609G/+}$ mice showed comparable levels of platelet activation markers compared to the control group. (B—C) Higher expression of platelet activation markers JON/A, but not CD62p, was detected on platelets from progeric animals compared to the wild-type (WT) upon stimulation with ADP. *Lmna*$^{G609G/+}$ platelets showed significantly higher expression of both CD62P and JON/A upon stimulation with (D-E) CRP and (F) thrombin. n = 11–12 different animals per group. Results are evaluated by two-way ANOVA with Sidak's *post hoc* test. Results are presented as mean ± SD. $^{**}P < 0.01$; $^{****}P < 0.0001$.

as indicated by augmented circulating TAT complexes.

Cardiovascular complications such as myocardial infarction and stroke are the predominant cause of mortality in HGPS. Many clinical, post-mortem human autopsies and animal studies were conducted to gather robust characterization of CV disease in HGPS [25]. Notably, severe accelerated atherosclerosis is the most predominant feature

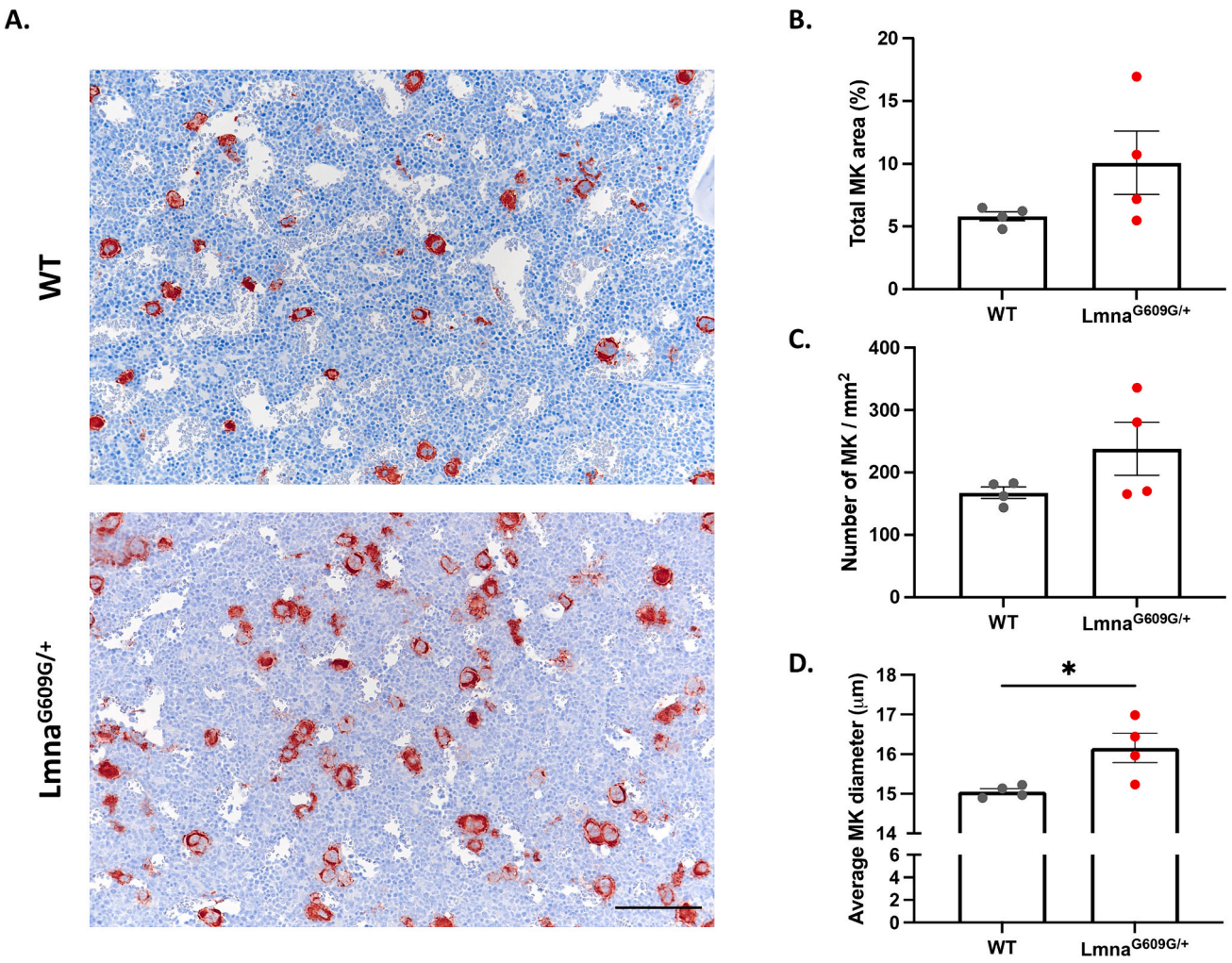

Fig. 5. Megakaryocyte assessment in the bone marrow of HGPS animals. (A) Representative pictures of bone marrow immunohistochemistry staining for integrin β3 (red stain) of wild-type and progeric mice, 200× magnification. Scale bar = 100 μm. (B—C) Progeric animals displayed an increasing trend in the total area and number of megakaryocytes in the bone marrow of the femur. (D) Megakaryocytes of *Lmna*$^{G609G/+}$mice are significantly larger compared to the control group. $n = 4$ different animals per group. Results are evaluated by unpaired two-tailed Student's t-test. Results are presented as mean ± SD. *$P < 0.05$. (For interpretation of the references to colour in this figure legend, the reader is referred to the web version of this article.)

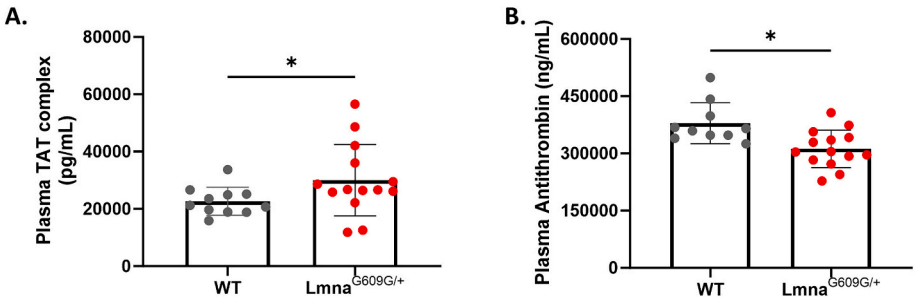

Fig. 6. Effect of *LMNA*^{G609G} mutation on thrombin and antithrombin III dynamics. (A) Plasma levels of thrombin antithrombin (TAT) complex increased in *Lmna*$^{G609G/+}$ mice, while, in parallel, showed lower antithrombin III levels (B) as compared to wild-type (WT) littermates. n = 11–12 different animals per group. Results are evaluated by unpaired two-tailed Student's t-test. Results are presented as mean ± SD. *$P < 0.05$.

observed in children with HGPS, who exhibit features such as evidence of calcification, inflammation as well as plaque rupture, and erosion [26,27]. Previous *ex vivo* and our *in vivo* observations also demonstrate more prominent vascular stiffness in animals bearing the *LMNA* mutation, which is in line with clinical findings recorded in children with HGPS [17,28]. Histological analysis revealed an increased collagen deposition, particularly collagen III, IV, V, and XII in the media layer of *Lmna*$^{G609G/G609G}$ animals' aorta [17]. In line with the previous observation, we show a higher expression of collagen III in the vascular tissue of *Lmna*$^{G609G/+}$ animals compared to the WT littermates. Even though flow-limiting stenosis that comes from generalized atherosclerosis and other pathological changes in the arterial wall were suggested to be critical factors leading to the premature death of HGPS patients [26,27], sudden thrombotic occlusion following plaque rupture or

thromboembolic events are also likely to play a role. Of note, an increased risk of thromboembolic complications was observed and associated with other *LMNA* mutations [29,30]. Indeed, in line with our initial hypothesis, we here showed that animals bearing the $LMNA^{G609G}$ mutation have a higher thrombotic potential, as demonstrated by decreased times to thrombotic occlusion. Considering the high rate of myocardial infarction and stroke in HGPS, such a pronounced pro-thrombotic condition presumably contributes to the mortality in this genetic disorder, besides other known factors.

Arterial thrombus formation is a complex and dynamic process involving three major players, *i.e.* the vessel wall, coagulation pathways, including the fibrinolytic system, and platelets [3,10]. Multiple coagulation and fibrinolysis mediators, including TF, PAI-1, and tPA, are predominantly expressed and released by vascular endothelial cells [18,31,32]. Previous observations demonstrated the detrimental effects of progerin on endothelial cell function, such as reduced nitric oxide production, defects in angiogenesis, and impaired shear stress response [33–35]. However, in this study, we observed that systemic and vascular levels of mediators involved in the activation of the coagulation cascade and fibrinolytic system TF, PAI-1, and tPA, were unaffected in HGPS mice. The irrelevance of the fibrinolytic system on the observed higher thrombogenicity in HGPS animals was further underscored by the unchanged thrombus embolization episodes and levels of fibrin degradation products, D-dimer.

Platelets are essential in arterial thrombus formation by tethering and adhering to the vessel wall upon injury, further inducing their activation and aggregation [36]. Higher platelet counts in patients with HGPS have been previously reported [37,38]. This phenotype was recorded in $Lmna^{G609G/G609G}$ mice [39] but not observed in our $Lmna^{G609G/+}$ animals. The exact reason for this discrepancy is not clear, yet clearly demonstrates the different phenotypes between species and between homozygous and heterozygous *LMNA* mutations. Nonetheless, FACS analysis showed that platelets of HGPS mice feature a higher reactivity to ADP, collagen, and thrombin. Following platelet activation, P-selectin is immediately expressed on the platelets' surface and shed into plasma as soluble P-selectin [40]. However, in the present study, soluble P-selectin levels did not differ between groups, which might be due to increased clearance by phagocytosis *in vivo* [41]. Moreover, Lamin A is involved in many cellular functions, including proteostasis [42]; hence, P-selectin shedding could be reduced withstanding a higher surface expression.

In the resting state, the expression of both platelet activation markers and platelet receptor density was not affected by the *LMNA* mutation, suggesting that the pro-thrombotic phenotype is unveiled upon stimulation only. Interestingly, we showed that GPVI receptor shedding was increased in platelets from animals bearing the $LMNA^{G609G}$ mutation. Of note, platelet surface receptor shedding is an irreversible proteolytic removal that elicits the downregulation of the platelet receptor density ligand-mediated platelet activation, generating a soluble fragment that is released into the circulation [42,43]. Previous studies report that elevated soluble GPVI is associated with atherothrombotic diseases, such as stroke [44] and thrombotic microangiopathy [45]. Hence, our finding might further indicate the higher thrombogenicity in HGPS. Collectively considered, our platelet study suggests that the *LMNA* mutation might lead to functional alteration of platelets, leading to higher responsiveness to specific stimuli.

In line with previous observations reporting the expression of lamin A in platelets and their secretome [46,47], we confirmed the presence of this nuclear protein in isolated mouse platelets. Considering that lamin A is a nuclear component, this finding is of interest since platelets are anucleate blood cells. Nonetheless, the difference between groups was not statistically significant. Besides, lamin A is highly expressed in megakaryocytes, the precursor cells of platelets, where progerin overexpression enhances cell polyploidization [48]. In line with this, our bone marrow analysis shows significantly larger megakaryocytes indicating higher cells' ploidy in progeric animals. Importantly, high ploidy megakaryocytes have been associated with the production of highly reactive platelets [49,50]. Therefore, our findings suggest the possible influence of the specific *LMNA* mutation on megakaryopoiesis, which might alter the platelet function in HGPS. Nonetheless, further studies are required to investigate the role of lamin A in megakaryopoiesis and platelet activity.

Activated platelets release their granules containing chemokines and clotting components, including TF and prothrombin, thus linking primary and secondary hemostasis and enhancing clot formation [51]. Furthermore, activated platelets exert a procoagulant activity by exposing aminophospholipid phosphatidylserine on their surface [52]. We show that platelets from HGPS animals expose more phosphatidylserine following activation, indicating higher procoagulant properties of these platelets. The externalization of membrane phospholipid acts as a catalytic scaffold on the platelet surface, facilitating the assembly of tenase (factors VIIIa, Ixa, and X) and prothrombinase (factors Va, Xa, and II) complexes, thus inducing further thrombin generation and further propagation of the coagulation process [52–54]. Consistently, we observed increased circulating levels of TAT complex in HGPS mice that underwent endothelial injury. TAT complex is a biomarker of intravascular thrombin formation, serving as a surrogate for an individual's hypercoagulability [55]. Thus, our finding confirms higher thrombin generation in HGPS animals, which might be aggravated by the increased platelet reactivity and augmented externalization of platelet phosphatidylserine upon activation. Of importance, previous evidence demonstrated that high levels of thrombin generate dense networks of relatively thin fibrin fibers that are more stable and resistant to fibrinolysis [56–58]. Therefore, the elevated thrombin generation in HGPS animals might not only further propagate clot formation *via* the positive feedback mechanism but also affect fibrin structure and architecture that are crucial for stable thrombus formation and eventually may intensify the arterial thrombus formation.

The TAT complex is formed as a thrombin-neutralizing activity by antithrombin III in a 1:1 ratio [59]. Yet, we observed a reduction of the plasma antithrombin III levels in $Lmna^{G609G/+}$ mice. In this respect, it should be noted that decreased antithrombin III levels, implying inadequate anticoagulation, can be either hereditary or acquired, resulting from decreased protein synthesis and/or increased consumption [59]. Given the swift antithrombin III consumption in the clot during acute thrombosis, the observed depleted plasma antithrombin III in progeric animals might result from ongoing consumption of this natural anticoagulant by increased thrombin generation [59,60]. Nevertheless, other mechanisms that might decrease antithrombin III levels cannot be entirely excluded. Hence, further investigation is needed to elucidate the effect of *LMNA* mutation on antithrombin III dynamics.

Regardless of the mechanism, the herein-reported data suggest for the first time that HGPS-related targeted *LMNA* mutation enhances platelet reactivity, which may aggravate thrombin generation and, eventually, arterial thrombosis. Collectively considered, mitigation of platelet reactivity may be suggested as a strategy to blunt fatal arterial thrombosis in children with HGPS.

4.1. Limitations

This study has some limitations that should be noted. First, our study indicates that the higher thrombogenicity in HGPS is mediated by augmented platelet reactivity accompanied by megakaryocyte alteration, yet the mechanisms were not explored. Therefore, further investigation on the detailed characterization of platelets and megakaryopoiesis in HGPS is needed. Furthermore, our findings are derived from animal data only and lack confirmation in patients with HGPS. However, it must be noted that obtaining suitable samples, such as freshly isolated platelets for platelet function assessment, from children suffering from a severe and extremely rare disease is technically and ethically challenging. Nevertheless, further confirmatory clinical investigations will be required.

5. Conclusions

In conclusion, this study provides evidence of an increased arterial thrombotic response in a mouse model of HGPS yielding the classic lamin A mutation observed in affected patients. The prothrombotic phenotype is mediated, at least in part, by enhanced platelet reactivity, which consequently augments thrombin generation. Our findings may provide mechanistic insight into the fatal incidence of major adverse CV events observed in children with HGPS beyond the well-established atherosclerotic burden. Given the wide clinical availability of antiplatelet agents, results from this study may lead to future clinical investigation to identify the most suitable antiplatelet regimen for children with HGPS in order to mitigate the mortality and morbidity in this rare syndrome.

Funding

The present work was supported by the Swiss National Science Foundation [310030_197510] to GGC, the Alfred and Annemarie von Sick Grants for Translational and Clinical Research Cardiology and Oncology to GGC, Jubiläumsstiftung von Swiss Life to YMP, and the Foundation for Cardiovascular Research–Zurich Heart House. GGC is the recipient of H.H. Sheikh Khalifa bin Hamad Al Thani Foundation Assistant Professorship at the Faculty of Medicine, University of Zurich.

CRediT authorship contribution statement

Yustina M. Puspitasari: Writing – original draft, Methodology, Investigation, Funding acquisition, Formal analysis, Data curation, Conceptualization. **Stefano Ministrini:** Writing – review & editing, Data curation. **Jiaying Han:** Writing – review & editing, Methodology, Formal analysis. **Caroline Karch:** Data curation. **Francesco Prisco:** Writing – review & editing, Visualization, Methodology, Data curation. **Luca Liberale:** Writing – review & editing, Conceptualization. **Susan Bengs:** Writing – review & editing, Resources. **Alexander Akhmedov:** Writing – review & editing, Resources. **Fabrizio Montecucco:** Writing – review & editing. **Jürg H. Beer:** Writing – review & editing. **Thomas F. Lüscher:** Writing – review & editing. **Dario Bongiovanni:** Writing – review & editing, Validation, Methodology. **Giovanni G. Camici:** Writing – review & editing, Supervision, Funding acquisition, Conceptualization.

Declaration of competing interest

The authors declare the following financial interests/personal relationships which may be considered as potential competing interests: Yustina M Puspitasari reports financial support was provided by Swiss Life Group. Giovanni G Camici reports financial support was provided by Swiss National Science Foundation. Luca Liberale reports a relationship with Daiichi Sankyo Inc. that includes: speaking and lecture fees. Giovanni G Camici reports a relationship with Sovida Solutions that includes: consulting or advisory. Thomas F Luescher reports a relationship with AstraZeneca Pharmaceuticals LP that includes: funding grants. Thomas F Luescher reports a relationship with Abbott that includes: funding grants. Thomas F Luescher reports a relationship with Amgen Inc. that includes: funding grants. Thomas F Luescher reports a relationship with Bayer HealthCare Pharmaceuticals Inc. that includes: funding grants. Thomas F Luescher reports a relationship with Boehringer Ingelheim GmbH that includes: funding grants. Thomas F Luescher reports a relationship with Daiichi Sankyo Inc. that includes: funding grants. Thomas F Luescher reports a relationship with Eli Lilly and Company that includes: funding grants. Thomas F Luescher reports a relationship with Novartis Pharmaceuticals Corporation that includes: funding grants. Thomas F Luescher reports a relationship with Novo Nordisk Inc. that includes: funding grants. Thomas F Luescher reports a relationship with Roche that includes: funding grants. Thomas F Luescher reports a relationship with Sanofi that includes: funding grants. Thomas F Luescher reports a relationship with Vifor Pharma Switzerland SA that includes: funding grants. Giovanni G Camici has patent #WO/2020/226993 pending to University of Zurich. Luca Liberale has patent #WO/2020/226993 pending to University of Zurich. If there are other authors, they declare that they have no known competing financial interests or personal relationships that could have appeared to influence the work reported in this paper.

Acknowledgments

We are grateful to the technical staff in the Histology Laboratory, Institute of Veterinary Pathology, Vetsuisse Faculty, University of Zurich (IVPZ), for excellent technical support.

Disclosures

LL and GGC are coinventors on the International Patent WO/2020/226993 filed in April 2020. The patent relates to the use of antibodies which specifically bind IL-1α to reduce various sequelae of ischemia-reperfusion injury to the central nervous system. GGC is a consultant to Sovida Solutions Limited. TFL has no conflicts related to this manuscript. Outside the work, he received unrestricted research and education grants from Abbott, Amgen, AstraZeneca, Bayer HealthCare, Boehringer Ingelheim, Daichi-Sankyo, Eli Lilly, Novartis, Novo Nordisk, Roche Diagnostics, Sanofi and Vifor. LL reports speaker fees outside of this work from Daichi-Sankyo. The other authors report no conflict of interest.

Appendix A. Supplementary data

Supplementary data to this article can be found online at https://doi.org/10.1016/j.thromres.2024.109100.

References

[1] F. Paneni, C. Diaz Cañestro, P. Libby, T.F. Lüscher, G.G. Camici, The aging cardiovascular system: understanding it at the cellular and clinical levels, J. Am. Coll. Cardiol. 69 (2017) 1952–1967, https://doi.org/10.1016/j.jacc.2017.01.064.
[2] R.H. Olie, P.E.J. van der Meijden, H. ten Cate, The coagulation system in atherothrombosis: implications for new therapeutic strategies, Res. Pract. Thromb. Haemost. 2 (2018) 188–198, https://doi.org/10.1002/rth2.12080.
[3] G. Lippi, M. Franchini, G. Targher, Arterial thrombus formation in cardiovascular disease, Nat. Rev. Cardiol. 8 (2011) 502–512, https://doi.org/10.1038/nrcardio.2011.91.
[4] F.G. Osorio, C.L. Navarro, J. Cadiñanos, I.C. López-Mejía, P.M. Quirós, C. Bartoli, J. Rivera, J. Tazi, G. Guzmán, I. Varela, D. Depetris, F. de Carlos, J. Cobo, V. Andrés, A. De Sandre-Giovannoli, J.M.P. Freije, N. Lévy, C. López-Otín, Splicing-Directed Therapy in a New Mouse Model of Human Accelerated Aging, Sci Transl Med 3, 2011, https://doi.org/10.1126/scitranslmed.3002847.
[5] A. Zaghini, G. Sarli, C. Barboni, M. Sanapo, V. Pellegrino, A. Diana, N. Linta, J. Rambaldi, M. D'Apice, M. Murdocca, M. Baleani, F. Baruffaldi, R. Fognani, R. Mecca, A. Festa, S. Papparella, O. Paciello, F. Prisco, C. Capanni, M. Loi, E. Schena, G. Lattanzi, S. Squarzoni, Long Term Breeding of the Lmna G609G Progeric Mouse: Characterization of Homozygous and Heterozygous Models, Exp Gerontol 130, 2020, https://doi.org/10.1016/J.EXGER.2019.110784.
[6] S. Gonzalo, R. Kreienkamp, P. Askjaer, Hutchinson-Gilford Progeria Syndrome: a premature aging disease caused by LMNA gene mutations, Ageing Res. Rev. 33 (2017) 18–29, https://doi.org/10.1016/j.arr.2016.06.007.
[7] L.B. Gordon, F.G. Rothman, C. López-Otín, T. Misteli, Progeria: a paradigm for translational medicine, Cell 156 (2014) 400, https://doi.org/10.1016/J.CELL.2013.12.028.
[8] J.E. May, S. Moll, Unexplained arterial thrombosis: approach to diagnosis and treatment, Hematology 2021 (2021) 76–84, https://doi.org/10.1182/hematology.2021000235.
[9] L. Liberale, A. Akhmedov, N.I. Vlachogiannis, N.R. Bonetti, V. Nageswaran, M. X. Miranda, Y.M. Puspitasari, L. Schwarz, S. Costantino, F. Paneni, J.H. Beer, F. Ruschitzka, F. Montecucco, T.F. Lüscher, K. Stamatelopoulos, K. Stellos, G. G. Camici, Sirtuin 5 promotes arterial thrombosis by blunting the fibrinolytic system, Cardiovasc. Res. (2020), https://doi.org/10.1093/cvr/cvaa268.
[10] L. Liberale, Y.M. Puspitasari, S. Ministrini, A. Akhmedov, S. Kraler, N.R. Bonetti, G. Beer, A. Vukolic, D. Bongiovanni, J. Han, K. Kirmes, I. Bernlochner, J. Pelisek, J. H. Beer, Z.-G. Jin, D. Pedicino, G. Liuzzo, K. Stellos, F. Montecucco, F. Crea, T. F. Lüscher, G.G. Camici, JCAD promotes arterial thrombosis through PI3K/Akt

modulation: a translational study, Eur. Heart J. (2022), https://doi.org/10.1093/EURHEARTJ/EHAC641.
[11] L. Liberale, S. Kraler, Y.M. Puspitasari, N.R. Bonetti, A. Akhmedov, S. Ministrini, F. Montecucco, N. Marx, M. Lehrke, N.U.K. Hartmann, J.H. Beer, F.A. Wenzl, F. Paneni, T.F. Lüscher, G.G. Camici, SGLT-2 inhibition by empagliflozin has no effect on experimental arterial thrombosis in a murine model of low-grade inflammation, Cardiovasc. Res. (2022), https://doi.org/10.1093/CVR/CVAC126.
[12] C. Diaz-Canestro, Y.M. Puspitasari, L. Liberale, T.J. Guzik, A.J. Flammer, N. R. Bonetti, P. Wüst, S. Costantino, F. Paneni, A. Akhmedov, Z. Varga, S. Ministrini, J.H. Beer, F. Ruschitzka, M. Hermann, T.F. Lüscher, I. Sudano, G.G. Camici, MMP-2 knockdown blunts age-dependent carotid stiffness by decreasing elastin degradation and augmenting eNOS activation, Cardiovasc. Res. (2021), https://doi.org/10.1093/CVR/CVAB300.
[13] M. Klug, K. Kirmes, J. Han, O. Lazareva, M. Rosenbaum, G. Viggiani, M. von Scheidt, J. Ruland, J. Baumbach, G. Condorelli, K.-L. Laugwitz, M. List, I. Bernlochner, D. Bongiovanni, Mass cytometry of platelet-rich plasma: a new approach to analyze platelet surface expression and reactivity, Platelets 33 (2022) 841–848, https://doi.org/10.1080/09537104.2021.2009453.
[14] I. Bernlochner, M. Klug, D. Larasati, M. Von Scheidt, D. Santovito, M. Hristov, C. Weber, K.-L. Laugwitz, D. Bongiovanni, Sorting and magnetic-based isolation of reticulated platelets from peripheral blood, Platelets 32 (2021) 113–119, https://doi.org/10.1080/09537104.2020.1724923.
[15] L. Liberale, A. Akhmedov, N.I. Vlachogiannis, N.R. Bonetti, V. Nageswaran, M. X. Miranda, Y.M. Puspitasari, L. Schwarz, S. Costantino, F. Paneni, J.H. Beer, F. Ruschitzka, F. Montecucco, T.F. Lüscher, K. Stamatelopoulos, K. Stellos, G. G. Camici, Sirtuin 5 promotes arterial thrombosis by blunting the fibrinolytic system, Cardiovasc. Res. 117 (2021) 2275–2288, https://doi.org/10.1093/cvr/cvaa268.
[16] S. Stivala, S. Gobbato, N. Bonetti, G.G. Camici, T.F. Lüscher, J.H. Beer, Dietary alpha-linolenic acid reduces platelet activation and collagen-mediated cell adhesion in sickle cell disease mice, J. Thromb. Haemost. 20 (2022) 375–386, https://doi.org/10.1111/jth.15581.
[17] L. Del Campo, A. Sánchez-López, M. Salaices, R.A. von Kleeck, E. Expósito, C. González-Gómez, L. Cussó, G. Guzmán-Martínez, J. Ruiz-Cabello, M. Desco, R. K. Assoian, A.M. Briones, V. Andrés, Vascular smooth muscle cell-specific progerin expression in a mouse model of Hutchinson-Gilford progeria syndrome promotes arterial stiffness: therapeutic effect of dietary nitrite, Aging Cell 18 (2019) e12936, https://doi.org/10.1111/acel.12936.
[18] J. Steffel, T.F. Lüscher, F.C. Tanner, Tissue factor in cardiovascular diseases, Circulation 113 (2006) 722–731, https://doi.org/10.1161/CIRCULATIONAHA.105.567297.
[19] L.G. Maxwell, S.R. Goodwin, T.J. Mancuso, V.C. Baum, A.L. Zuckerberg, P. G. Morgan, E.K. Motoyama, P.J. Davis, K.J. Sullivan, Systemic disorders, in: Smith's Anesthesia for Infants and Children, Elsevier, 2011, pp. 1098–1182, https://doi.org/10.1016/B978-0-323-06612-9.00036-5.
[20] H. Lin, L. Xu, S. Yu, W. Hong, M. Huang, P. Xu, Therapeutics targeting the fibrinolytic system, Exp. Mol. Med. 52 (2020) 367–379, https://doi.org/10.1038/s12276-020-0397-x.
[21] F. Peyvandi, I. Garagiola, L. Baronciani, Role of von Willebrand factor in the haemostasis, Blood Transfus. 9 (Suppl. 2) (2011) s3–s8, https://doi.org/10.2450/2011.002S.
[22] R.M.W. de Laat-Kremers, Q. Yan, M. Ninivaggi, M. de Maat, B. de Laat, Deciphering the coagulation profile through the dynamics of thrombin activity, Sci. Rep. 10 (2020) 12544, https://doi.org/10.1038/s41598-020-69415-y.
[23] E. De Candia, Mechanisms of platelet activation by thrombin: a short history, Thromb. Res. 129 (2012) 250–256, https://doi.org/10.1016/j.thromres.2011.11.001.
[24] G.E. Rivard, K.E. Brummel-Ziedins, K.G. Mann, L. Fan, A. Hofer, E. Cohen, Evaluation of the profile of thrombin generation during the process of whole blood clotting as assessed by thrombelastography, J. Thromb. Haemost. 3 (2005) 2039–2043, https://doi.org/10.1111/j.1538-7836.2005.01513.x.
[25] M. Gerhard-Herman, L.B. Smoot, N. Wake, M.W. Kieran, M.E. Kleinman, D. T. Miller, A. Schwartzman, A. Giobbie-Hurder, D. Neuberg, L.B. Gordon, Mechanisms of premature vascular aging in children with Hutchinson-Gilford progeria syndrome, Hypertension 59 (2012) 92–97, https://doi.org/10.1161/HYPERTENSIONAHA.111.180919.
[26] M.R. Hamczyk, R. Villa-Bellosta, P. Gonzalo, M.J. Andrés-Manzano, P. Nogales, J. F. Bentzon, C. López-Otín, V. Andrés, Vascular smooth muscle–specific progerin expression accelerates atherosclerosis and death in a mouse model of Hutchinson-Gilford Progeria Syndrome, Circulation 138 (2018) 266–282, https://doi.org/10.1161/CIRCULATIONAHA.117.030856.
[27] M. Olive, I. Harten, R. Mitchell, J.K. Beers, K. Djabali, K. Cao, M.R. Erdos, C. Blair, B. Funke, L. Smoot, M. Gerhard-Herman, J.T. Machan, R. Kutys, R. Virmani, F. S. Collins, T.N. Wight, E.G. Nabel, L.B. Gordon, Cardiovascular pathology in Hutchinson-Gilford progeria: correlation with the vascular pathology of aging, Arterioscler. Thromb. Vasc. Biol. 30 (2010) 2301–2309, https://doi.org/10.1161/ATVBAHA.110.209460.
[28] M. Gerhard-Herman, L.B. Smoot, N. Wake, M.W. Kieran, M.E. Kleinman, D. T. Miller, A. Schwartzman, A. Giobbie-Hurder, D. Neuberg, L.B. Gordon, Mechanisms of premature vascular aging in children with Hutchinson-Gilford progeria syndrome, Hypertension 59 (2012) 92–97, https://doi.org/10.1161/HYPERTENSIONAHA.111.180919.
[29] G. Boriani, M. Gallina, L. Merlini, G. Bonne, D. Toniolo, S. Amati, M. Biffi, C. Martignani, L. Frabetti, M. Bonvicini, C. Rapezzi, A. Branzi, Clinical relevance of atrial fibrillation/flutter, stroke, pacemaker implant, and heart failure in Emery-Dreifuss muscular dystrophy, Stroke 34 (2003) 901–908, https://doi.org/10.1161/01.STR.0000064322.47667.49.
[30] I.A.W. Van Rijsingen, A. Bakker, D. Azim, J.F. Hermans-Van Ast, A.J. Van Der Kooi, J.P. Van Tintelen, M.P. Van Den Berg, I. Christiaans, R.H. Lekanne Dit Deprez, A.A. M. Wilde, A.H. Zwinderman, J.C.M. Meijers, A.E. Grootemaat, R. Nieuwland, Y. M. Pinto, S.J. Pinto-Sietsma, Lamin A/C mutation is independently associated with an increased risk of arterial and venous thromboembolic complications, Int. J. Cardiol. 168 (2013) 472–477, https://doi.org/10.1016/J.IJCARD.2012.09.118.
[31] M. Cesari, M. Pahor, R.A. Incalzi, REVIEW: Plasminogen Activator Inhibitor-1 (PAI-1): a key factor linking fibrinolysis and age-related subclinical and clinical conditions, Cardiovasc. Ther. 28 (2010), https://doi.org/10.1111/j.1755-5922.2010.00171.x.
[32] C. Seillier, P. Hélie, G. Petit, D. Vivien, D. Clemente, B. Le Mauff, F. Docagne, O. Toutirais, Roles of the tissue-type plasminogen activator in immune response, Cell. Immunol. 371 (2022) 104451, https://doi.org/10.1016/j.cellimm.2021.104451.
[33] Q. Xu, A. Mojiri, L. Boulahouache, E. Morales, B.K. Walther, J.P. Cooke, Vascular senescence in progeria: role of endothelial dysfunction, Eur. Heart J. Open 2 (2022), https://doi.org/10.1093/ehjopen/oeac047.
[34] S. Osmanagic-Myers, A. Kiss, C. Manakanatas, O. Hamza, F. Sedlmayer, P.L. Szabo, I. Fischer, P. Fichtinger, B.K. Podesser, M. Eriksson, R. Foisner, Endothelial progerin expression causes cardiovascular pathology through an impaired mechanoresponse, J. Clin. Investig. 129 (2018) 531–545, https://doi.org/10.1172/JCI121297.
[35] G. Matrone, R.A. Thandavarayan, B.K. Walther, S. Meng, A. Mojiri, J.P. Cooke, Dysfunction of iPSC-derived endothelial cells in human Hutchinson–Gilford progeria syndrome, Cell Cycle 18 (2019) 2495–2508, https://doi.org/10.1080/15384101.2019.1651587.
[36] K. Broos, H.B. Feys, S.F. De Meyer, K. Vanhoorelbeke, H. Deckmyn, Platelets at work in primary hemostasis, Blood Rev. 25 (2011) 155–167, https://doi.org/10.1016/j.blre.2011.03.002.
[37] M.A. Merideth, L.B. Gordon, S. Clauss, V. Sachdev, A.C.M. Smith, M.B. Perry, C. C. Brewer, C. Zalewski, H.J. Kim, B. Solomon, B.P. Brooks, L.H. Gerber, M. L. Turner, D.L. Domingo, T.C. Hart, J. Graf, J.C. Reynolds, A. Gropman, J. A. Yanovski, M. Gerhard-Herman, F.S. Collins, E.G. Nabel, R.O. Cannon, W. A. Gahl, W.J. Introne, Phenotype and course of Hutchinson-Gilford progeria syndrome, N. Engl. J. Med. 358 (2008) 592–604, https://doi.org/10.1056/NEJMoa0706898.
[38] M. Díez-Díez, M. Amorós-Pérez, J. de la Barrera, E. Vázquez, A. Quintas, D. A. Pascual-Figal, A. Dopazo, F. Sánchez-Cabo, M.E. Kleinman, L.B. Gordon, V. Fuster, V. Andrés, J.J. Fuster, Clonal hematopoiesis is not prevalent in Hutchinson-Gilford progeria syndrome, Geroscience 45 (2023) 1231–1236, https://doi.org/10.1007/s11357-022-00607-2.
[39] Y.-H. Ho, R. del Toro, J. Rivera-Torres, J. Rak, C. Korn, A. García-García, D. Macías, C. González-Gómez, A. del Monte, M. Wittner, A.K. Waller, H.R. Foster, C. López-Otín, R.S. Johnson, C. Nerlov, C. Ghevaert, W. Vainchenker, F. Louache, V. Andrés, S. Méndez-Ferrer, Remodeling of bone marrow hematopoietic stem cell niches promotes myeloid cell expansion during premature or physiological aging, Cell Stem Cell 25 (2019) 407-418.e6, https://doi.org/10.1016/j.stem.2019.06.007.
[40] Y. Chen, G. Davis-Gorman, R.R. Watson, P.F. McDonagh, Platelet CD62p expression and microparticle formation in murine acquired immune deficiency syndrome and chronic ethanol consumption, Alcohol Alcohol. 38 (2003) 25–30, https://doi.org/10.1093/alcalc/agg013.
[41] A.A. Manfredi, G.A. Ramirez, C. Godino, A. Capobianco, A. Monno, S. Franchini, E. Tombetti, S. Corradetti, J.H.W. Distler, M.E. Bianchi, P. Rovere-Querini, N. Maugeri, Platelet phagocytosis via P-selectin glycoprotein ligand 1 and accumulation of microparticles in systemic sclerosis, Arthritis Rheum. 74 (2022) 318–328, https://doi.org/10.1002/art.41926.
[42] Z. Chen, N.K. Mondal, J. Ding, J. Gao, B.P. Griffith, Z.J. Wu, Shear-induced platelet receptor shedding by non-physiological high shear stress with short exposure time: glycoprotein Ibα and glycoprotein VI, Thromb. Res. 135 (2015) 692–698, https://doi.org/10.1016/j.thromres.2015.01.030.
[43] E.E. Gardiner, J.F. Arthur, M.L. Kahn, M.C. Berndt, R.K. Andrews, Regulation of platelet membrane levels of glycoprotein VI by a platelet-derived metalloproteinase, Blood 104 (2004) 3611–3617, https://doi.org/10.1182/blood-2004-04-1549.
[44] M. Al-Tamimi, E.E. Gardiner, J.Y. Thom, Y. Shen, M.N. Cooper, G.J. Hankey, M. C. Berndt, R.I. Baker, R.K. Andrews, Soluble glycoprotein VI is raised in the plasma of patients with acute ischemic stroke, Stroke 42 (2011) 498–500, https://doi.org/10.1161/STROKEAHA.110.602532.
[45] Y. Yamashita, K. Naitoh, H. Wada, M. Ikejiri, T. Mastumoto, K. Ohishi, Y. Hosaka, M. Nishikawa, N. Katayama, Elevated plasma levels of soluble platelet glycoprotein VI (GPVI) in patients with thrombotic microangiopathy, Thromb. Res. 133 (2014) 440–444, https://doi.org/10.1016/j.thromres.2013.11.023.
[46] B.A. Garcia, D.M. Smalley, J. Shabanowitz Cho, K. Ley, D.F. Hunt, The platelet microparticle proteome, J. Proteome Res. 4 (2005) 1516–1521, https://doi.org/10.1021/pr0500760.
[47] A. Della Corte, N. Maugeri, A. Pampuch, C. Cerletti, G. de Gaetano, D. Rotilio, Application of 2-dimensional difference gel electrophoresis (2D-DIGE) to the study of thrombin-activated human platelet secretome, Platelets 19 (2008) 43–50, https://doi.org/10.1080/09537100701609035.
[48] J.-W. Shin, K.R. Spinler, J. Swift, J.A. Chasis, N. Mohandas, D.E. Discher, Lamins regulate cell trafficking and lineage maturation of adult human hematopoietic cells, Proc. Natl. Acad. Sci. 110 (2013) 18892–18897, https://doi.org/10.1073/pnas.1304996110.

[49] J.F. Martin, S.D. Kristensen, A. Mathur, E.L. Grove, F.A. Choudry, The causal role of megakaryocyte–platelet hyperactivity in acute coronary syndromes, Nat. Rev. Cardiol. 9 (2012) 658–670, https://doi.org/10.1038/nrcardio.2012.131.
[50] V. Hancock, J.F. Martin, R. Lelchuk, The relationship between human megakaryocyte nuclear DNA content and gene expression, Br. J. Haematol. 85 (1993) 692–697, https://doi.org/10.1111/j.1365-2141.1993.tb03210.x.
[51] C.W. Smith, Release of α-granule contents during platelet activation, Platelets 33 (2022) 491–502, https://doi.org/10.1080/09537104.2021.1913576.
[52] E.C. Reddy, M.L. Rand, Procoagulant phosphatidylserine-exposing platelets in vitro and in vivo, Front. Cardiovasc. Med. 7 (2020), https://doi.org/10.3389/fcvm.2020.00015.
[53] S.M. Schoenwaelder, Y. Yuan, E.C. Josefsson, M.J. White, Y. Yao, K.D. Mason, L. A. O'Reilly, K.J. Henley, A. Ono, S. Hsiao, A. Willcox, A.W. Roberts, D.C.S. Huang, H.H. Salem, B.T. Kile, S.P. Jackson, Two distinct pathways regulate platelet phosphatidylserine exposure and procoagulant function, Blood 114 (2009) 663–666, https://doi.org/10.1182/blood-2009-01-200345.
[54] C. Tripisciano, R. Weiss, T. Eichhorn, A. Spittler, T. Heuser, M.B. Fischer, V. Weber, Different potential of extracellular vesicles to support thrombin generation: contributions of phosphatidylserine, tissue factor, and cellular origin, Sci. Rep. 7 (2017) 6522, https://doi.org/10.1038/s41598-017-03262-2.
[55] S. Fidan, M. Erkut, A.M. Cosar, Y. Yogun, A. Örem, M. Sönmez, M. Arslan, Higher thrombin-Antithrombin III complex levels May indicate severe acute pancreatitis, Dig. Dis. 36 (2018) 244–251, https://doi.org/10.1159/000485613.
[56] A.S. Wolberg, R.A. Campbell, Thrombin generation, fibrin clot formation and hemostasis, Transfus. Apher. Sci. 38 (2008) 15–23, https://doi.org/10.1016/j.transci.2007.12.005.
[57] D.A. Gorog, Z.A. Fayad, V. Fuster, Arterial thrombus stability, J. Am. Coll. Cardiol. 70 (2017) 2036–2047, https://doi.org/10.1016/j.jacc.2017.08.065.
[58] S. Kattula, J.R. Byrnes, A.S. Wolberg, Fibrinogen and Fibrin in Hemostasis and Thrombosis, Arterioscler Thromb Vasc Biol 37, 2017, https://doi.org/10.1161/ATVBAHA.117.308564.
[59] C.P.R. Walker, D. Royston, Thrombin generation and its inhibition: a review of the scientific basis and mechanism of action of anticoagulant therapies, Br. J. Anaesth. 88 (2002) 848–863, https://doi.org/10.1093/bja/88.6.848.
[60] E.F. Mammen, Antithrombin: its physiological importance and role in DIC, Semin. Thromb. Hemost. 24 (1998) 19–25, https://doi.org/10.1055/s-2007-995819.